Time dependent aggregation induced emission enhancement and study of molecular packing in closely related azo-phenol BODIPY species

Rajendra Prasad Paitandi, Roop Shikha Singh, Bhupendra Kumar Dwivedi, Vishwa Deepak Singh, and Daya Shankar Pandey*

Department of Chemistry, Institute of Science, Banaras Hindu University, Varanasi - 221005 (U.P.) India.

Contents

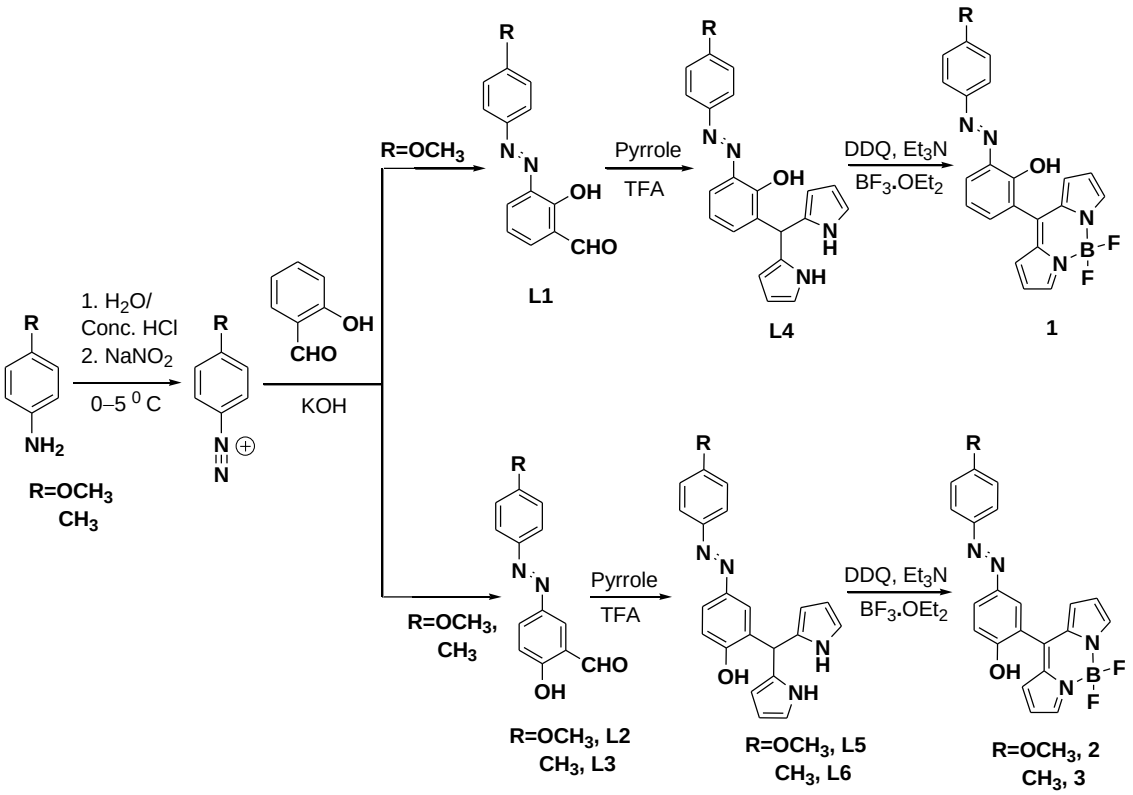

Scheme S1. Synthesis of **1**–**3**.

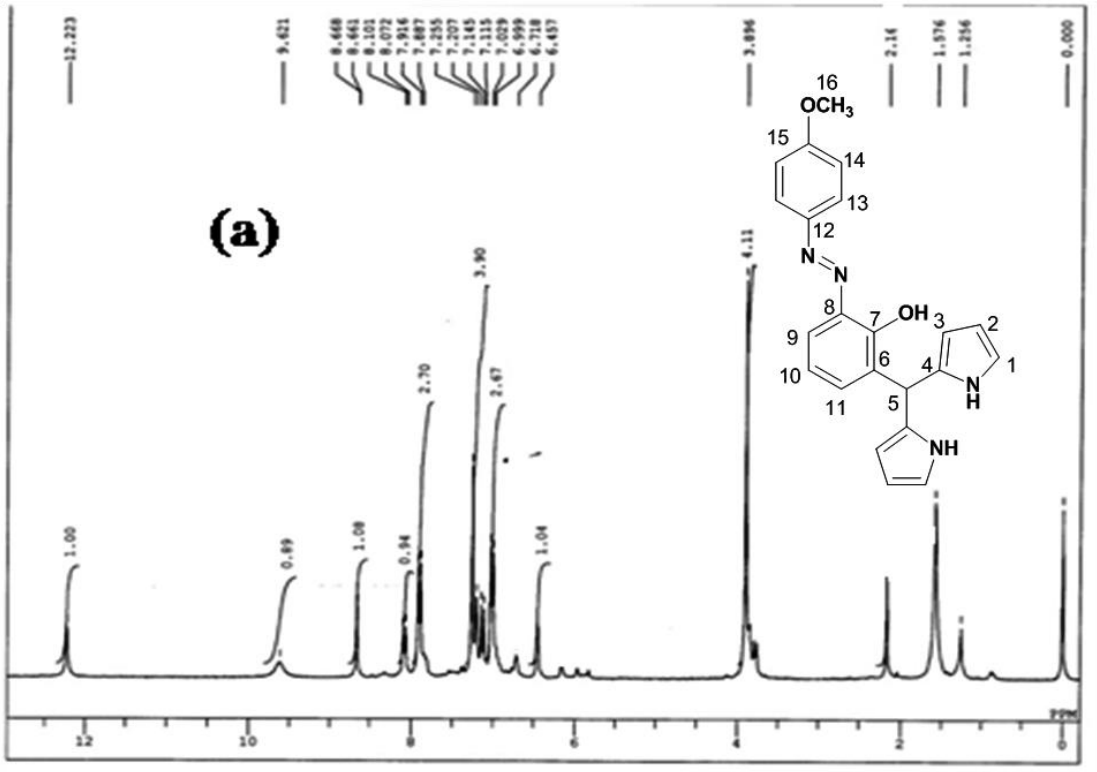

Fig. S1 ^{1}H (a) NMR spectra of **L4** in $CDCl_3$.

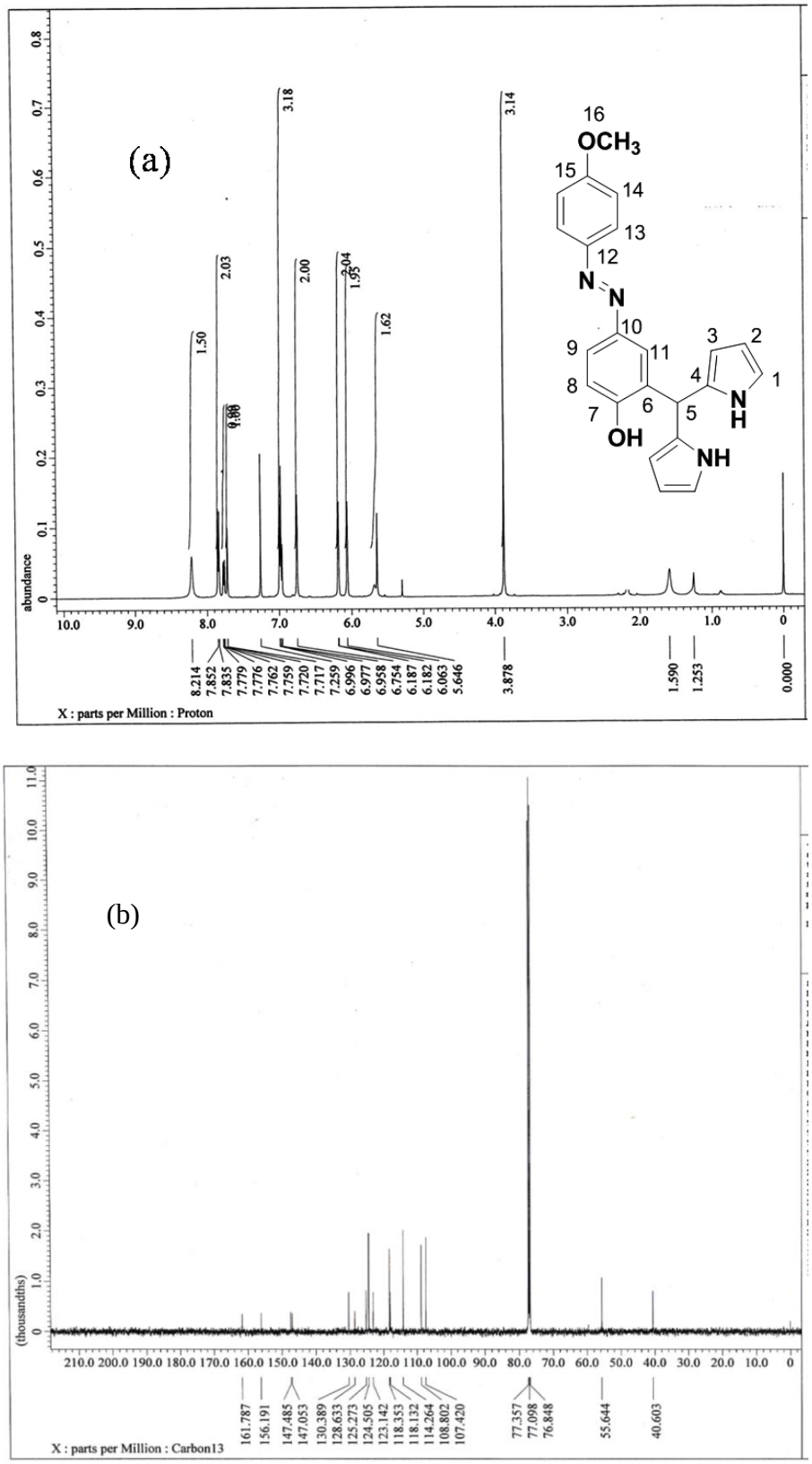

Fig. S2 ^{1}H (a) and ^{13}C (b) NMR spectra of **L5** in $CDCl_3$.

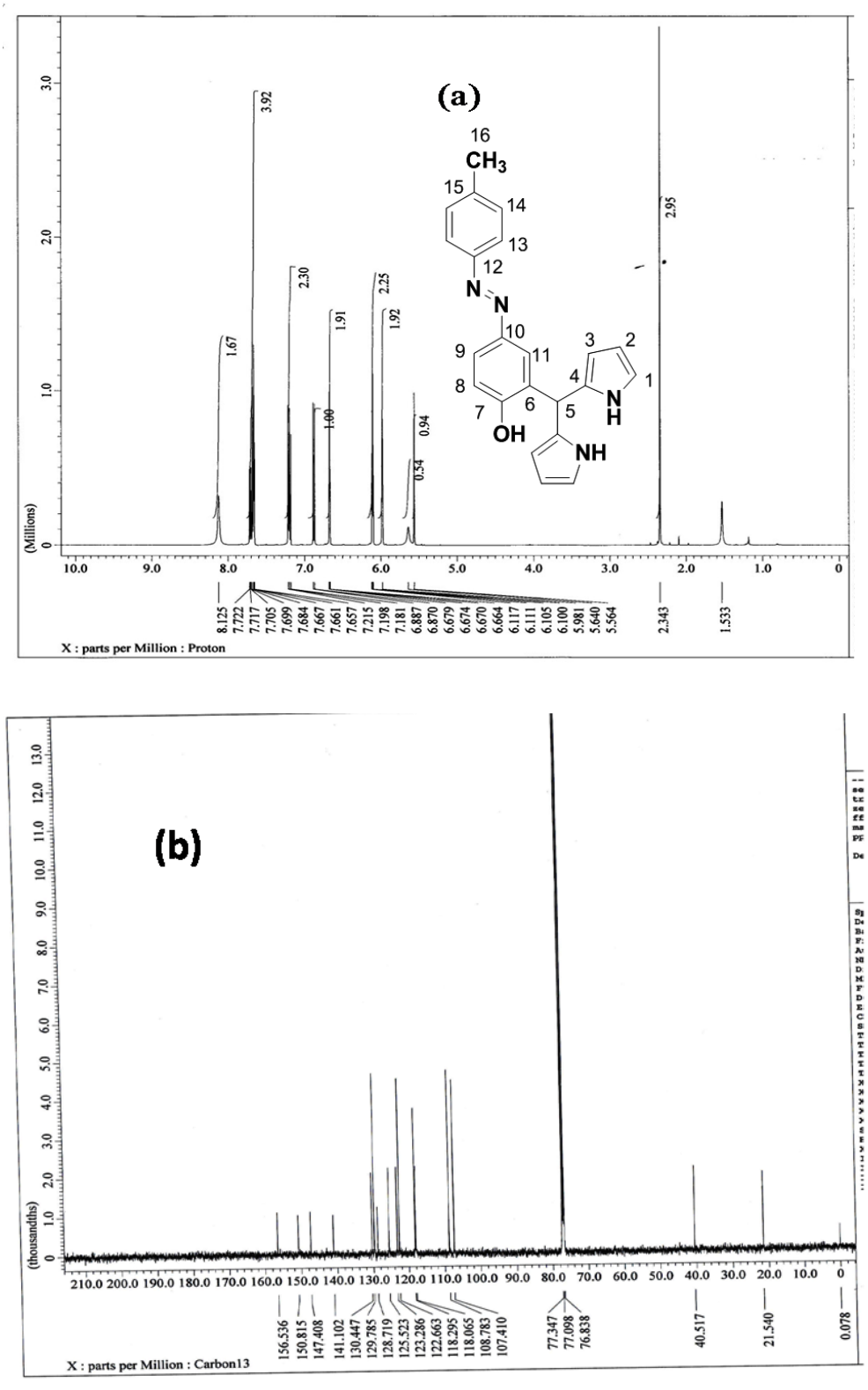

Fig. S3 ^{1}H (a) and ^{13}C (b) NMR spectra of **L6** in $CDCl_3$.

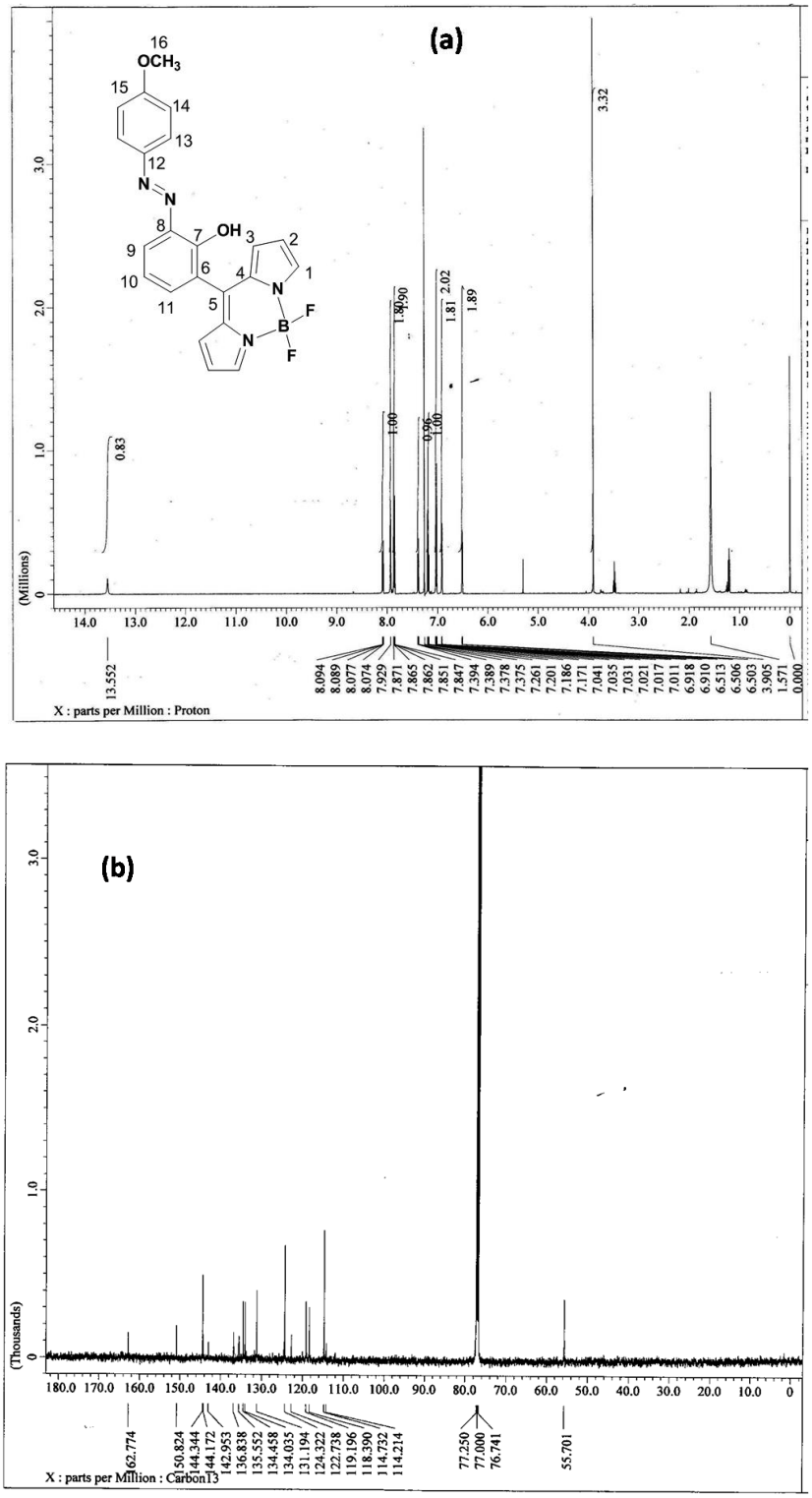

Fig. S4 ^{1}H (a) and ^{13}C (b) NMR spectra of **1** in $CDCl_3$.

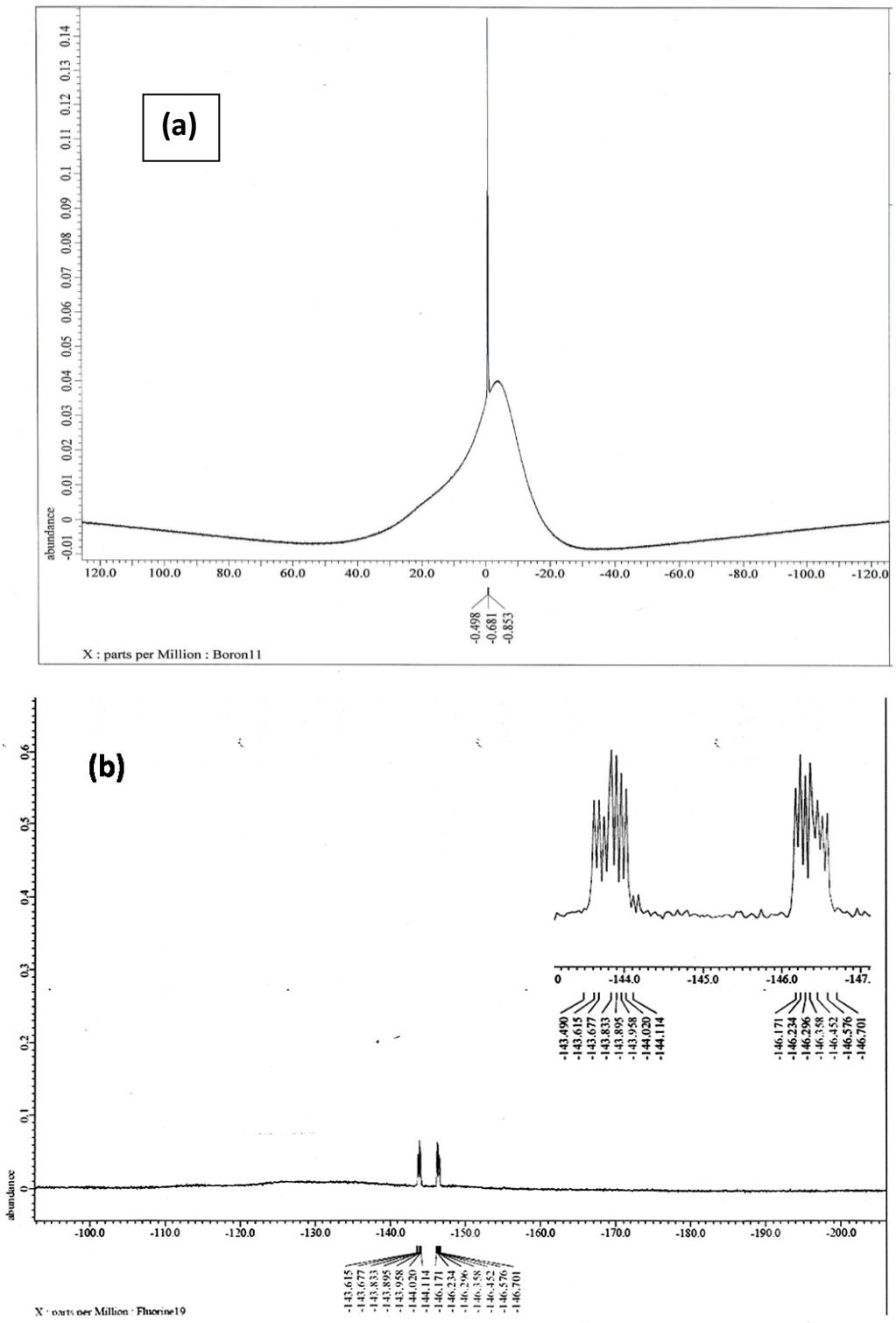

Fig. S5 ^{11}B (a) and ^{19}F (b) NMR spectra of **1** in $CDCl_3$.

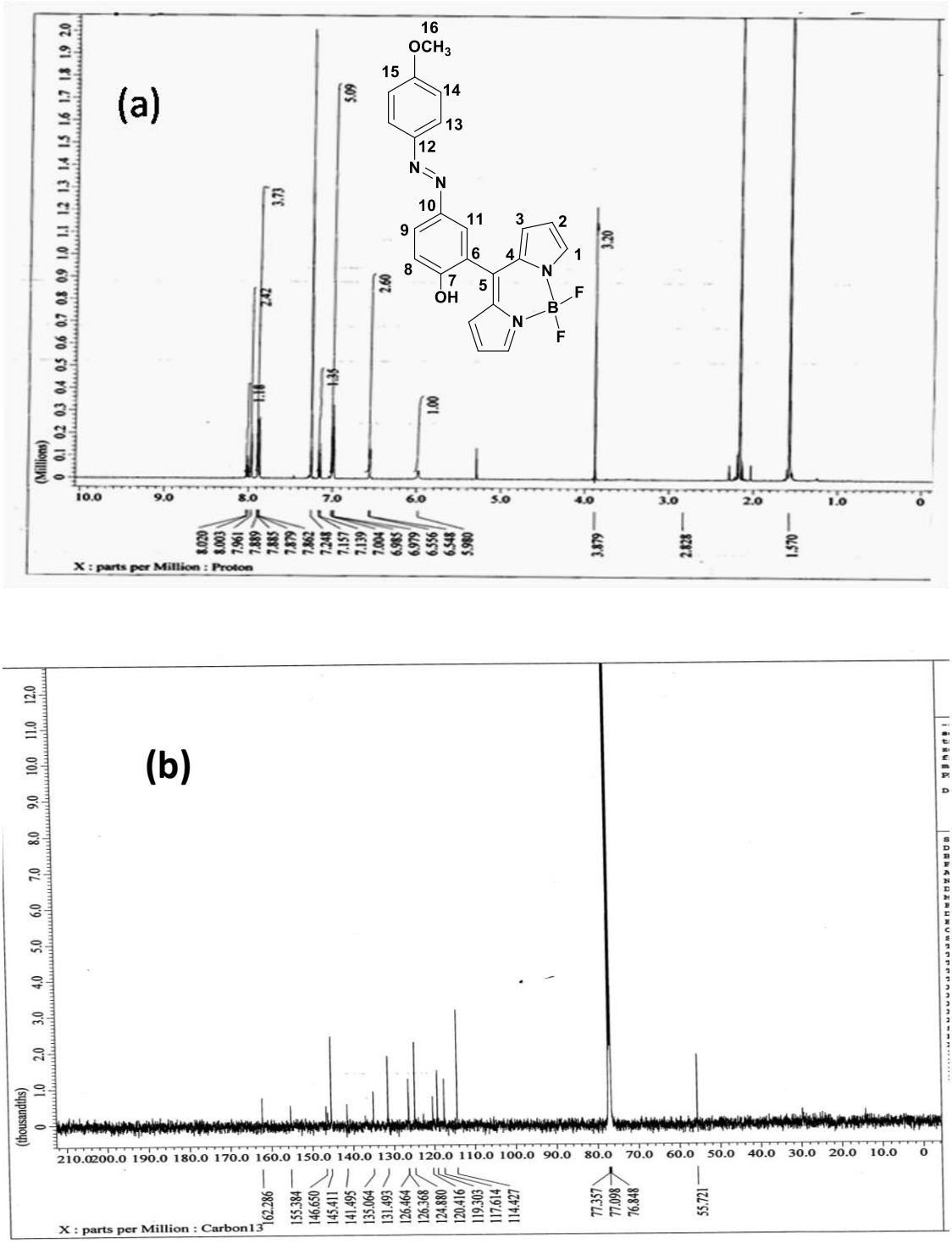

Fig. S6 ^{1}H (a) and ^{13}C (b) NMR spectra of **2** in $CDCl_3$.

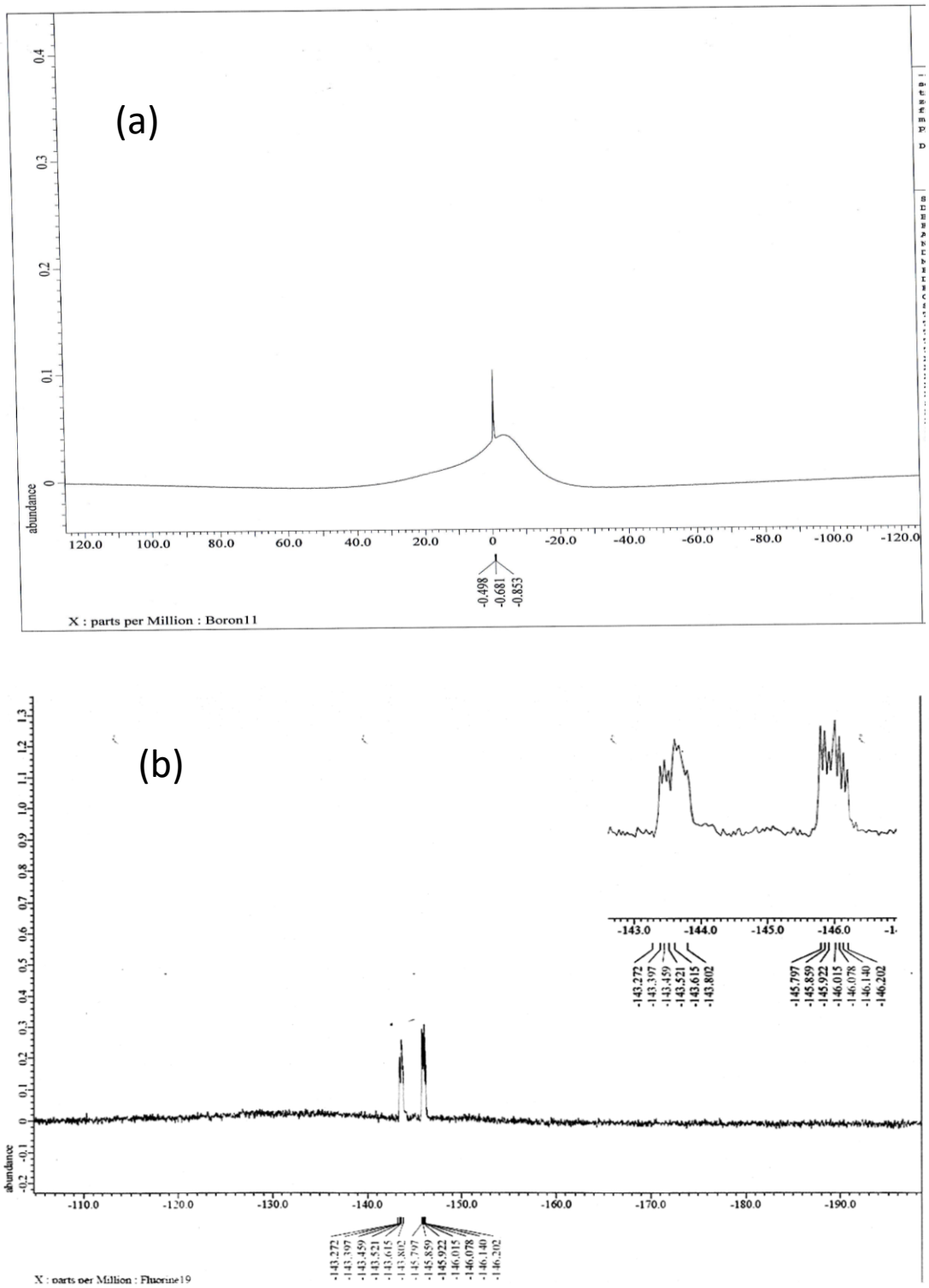

Fig. S7 ^{11}B (a) and ^{19}F (b) NMR spectra of **2** in $CDCl_3$.

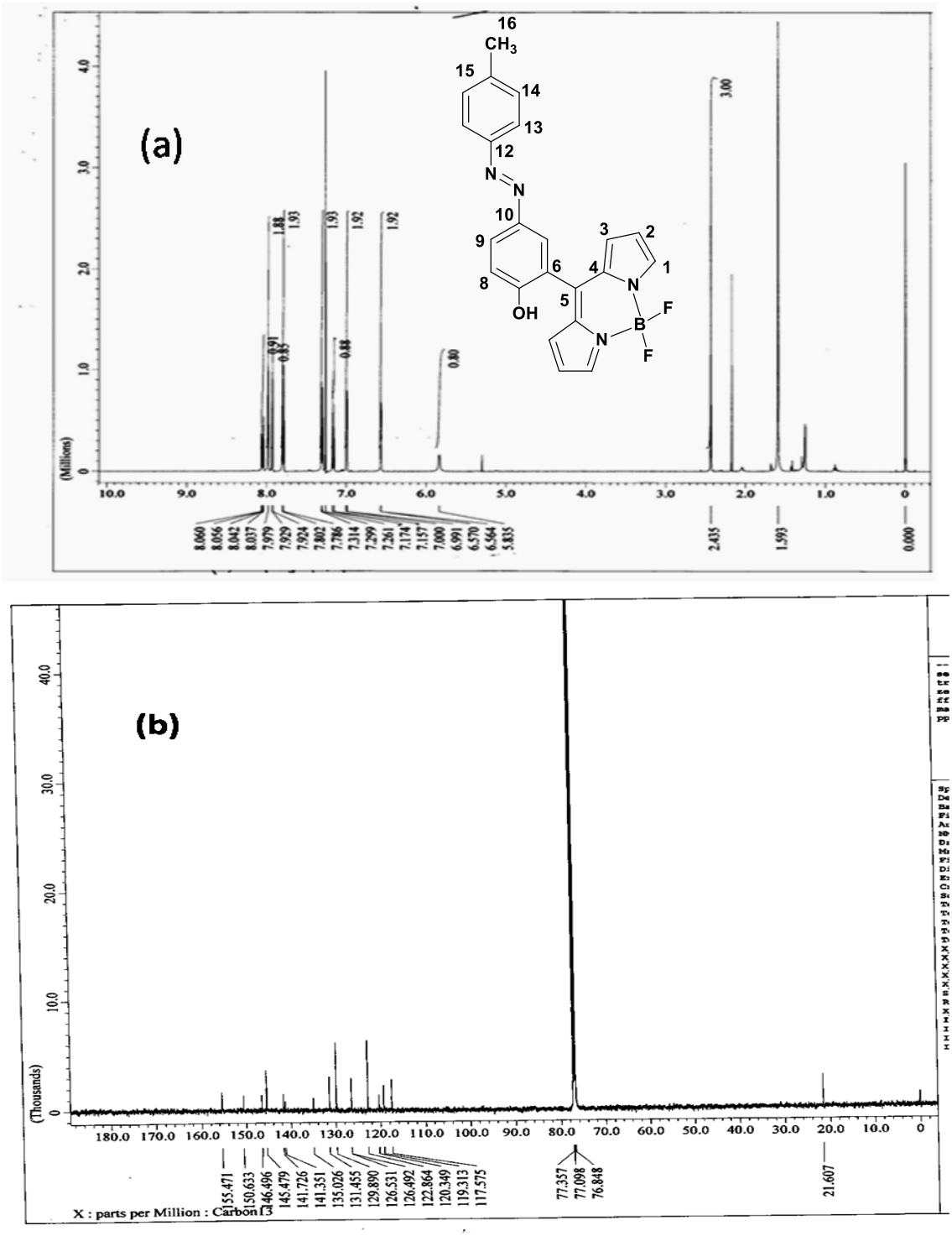

Fig. S8 ^{1}H (a) and ^{13}C (b) NMR spectra of **3** in $CDCl_3$.

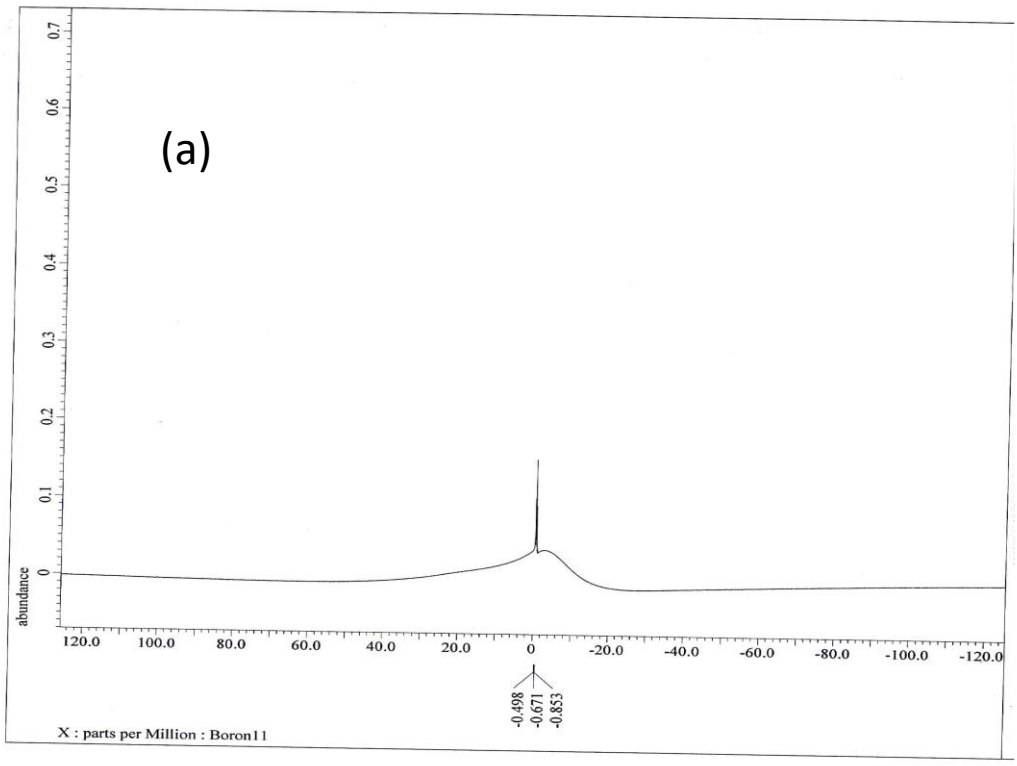

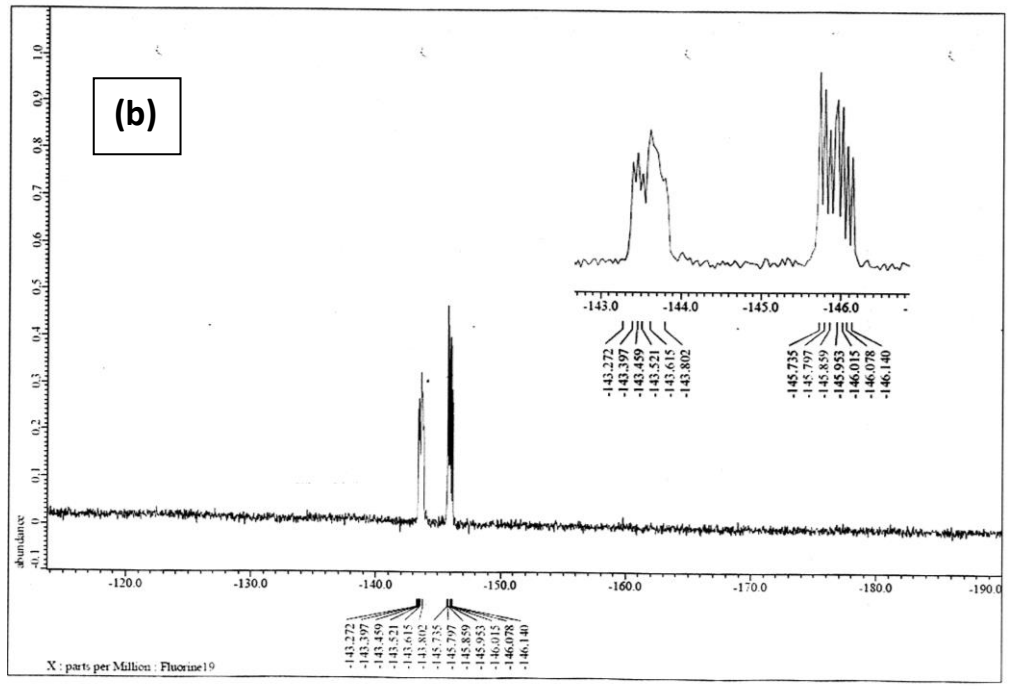

Fig. S9 ^{11}B (a) and ^{19}F (b) NMR spectra of **3** in $CDCl_3$.

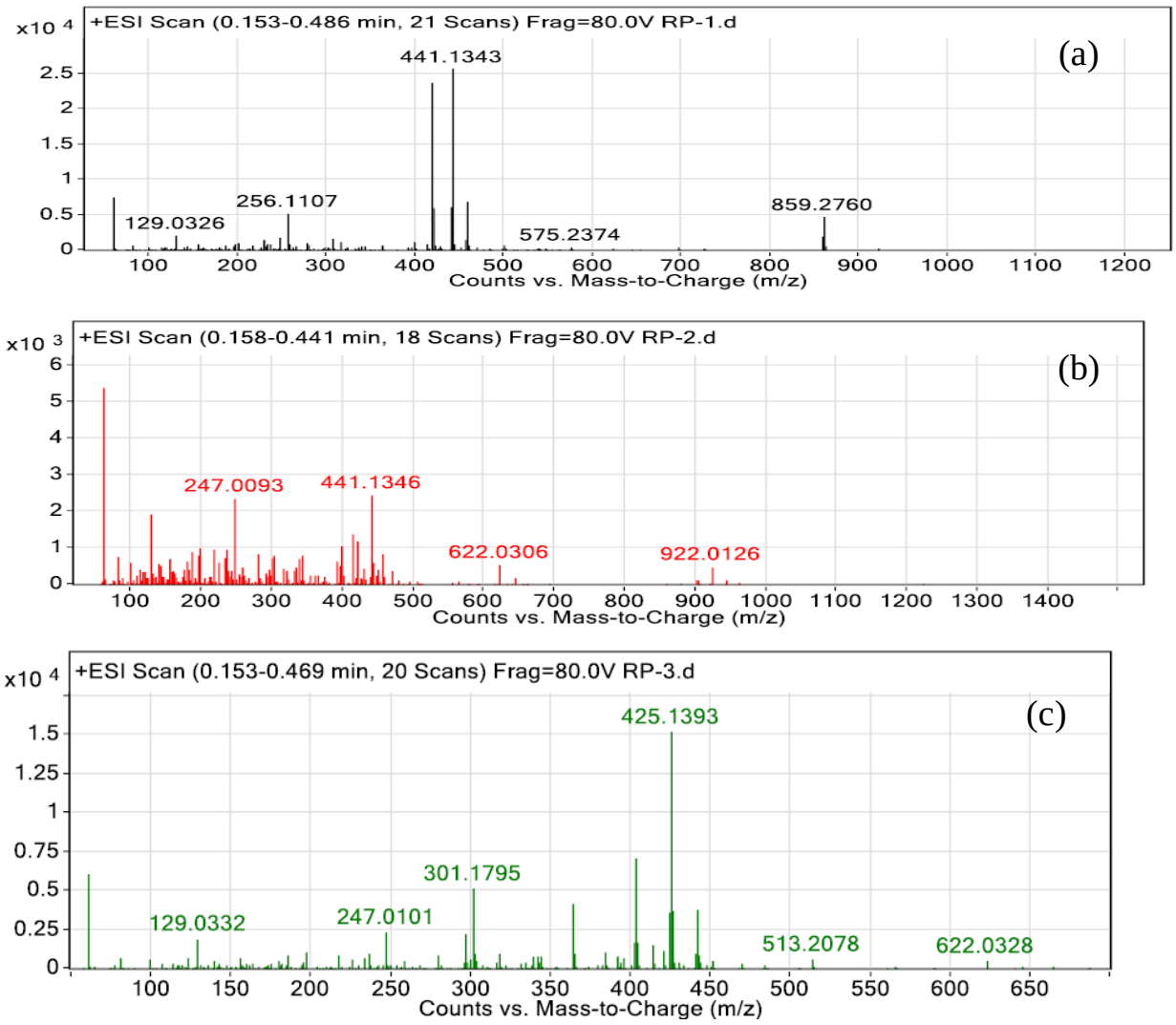

Fig. S10 HRMS spectra of **1–3** (a–c respectively).

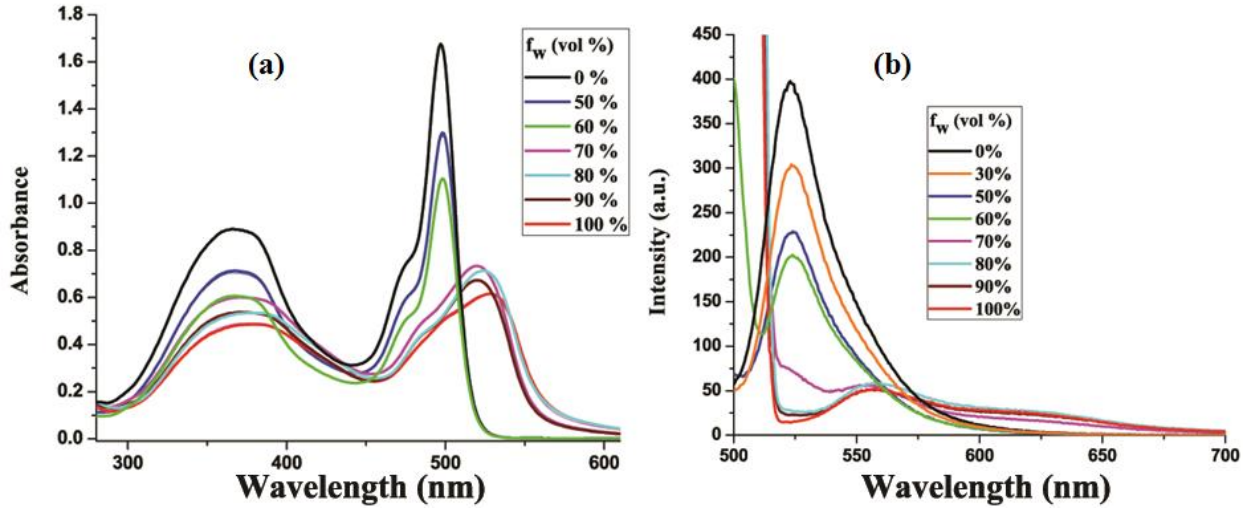

Fig. S11 UV-vis (a) and Fluorescence (b) spectra of **1** (*c*, 50 μM) in methanol/water mixture with different volume fractions of water (f_W).

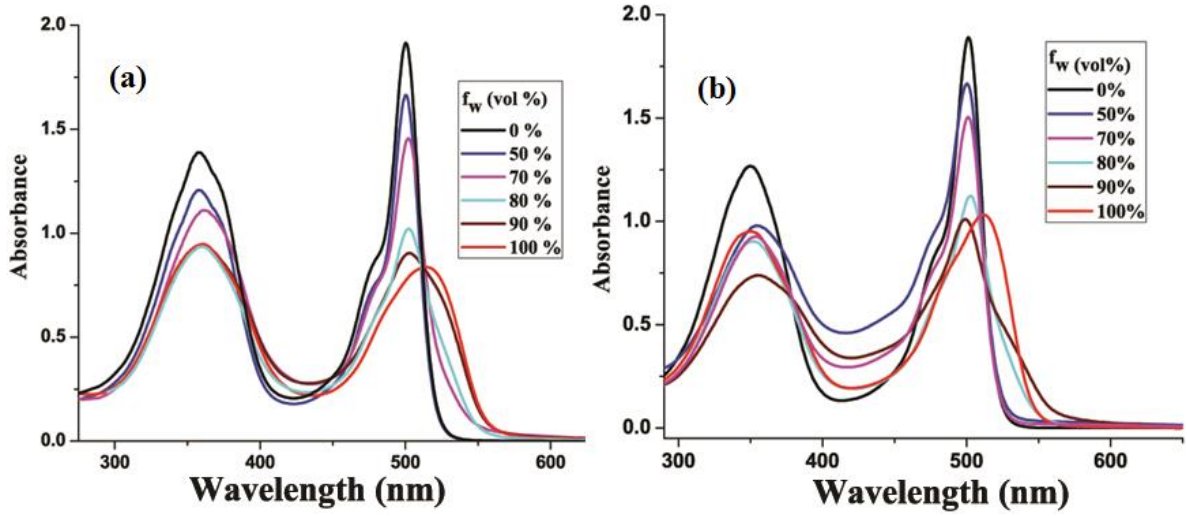

Fig. S12 UV-vis spectra of **2** (a) and **3** (b); (*c*, 50 μM) in methanol/water mixture with different volume fractions of water (f_W).

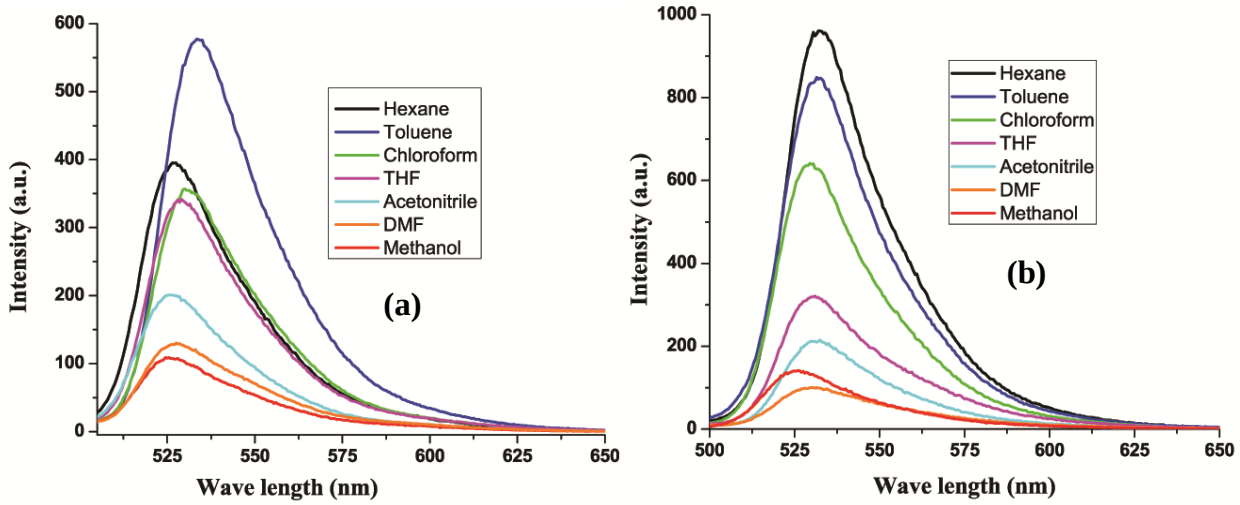

Fig. S13 Emission spectra of **2** (a) and **3** (b) in different solvents (*c*, 50 μM).

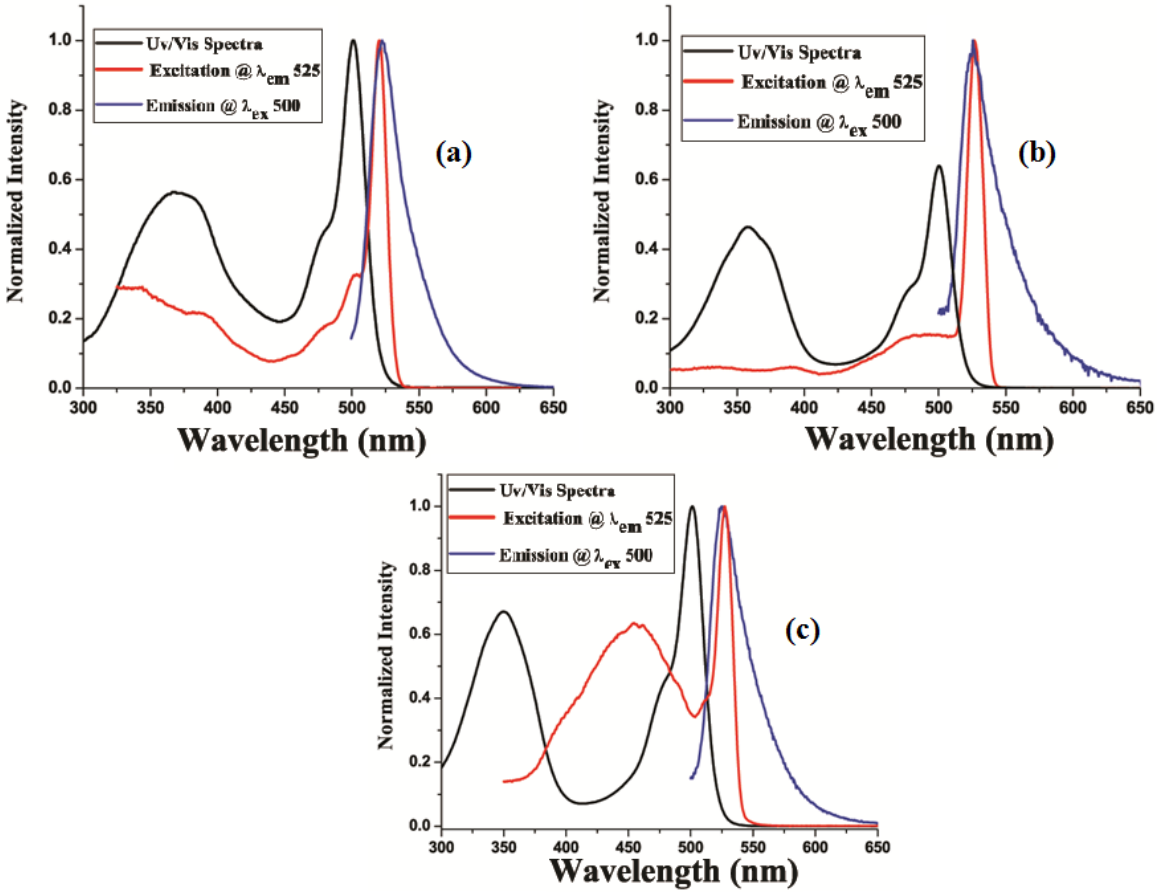

Fig. S14 Excitation spectra of compounds **1** (a), **2** (b) and **3** (c) compared with corresponding emission bands (λ_{ex} = 500 nm) and UV-vis spectra in methanol solution (*c*, 50 μM).

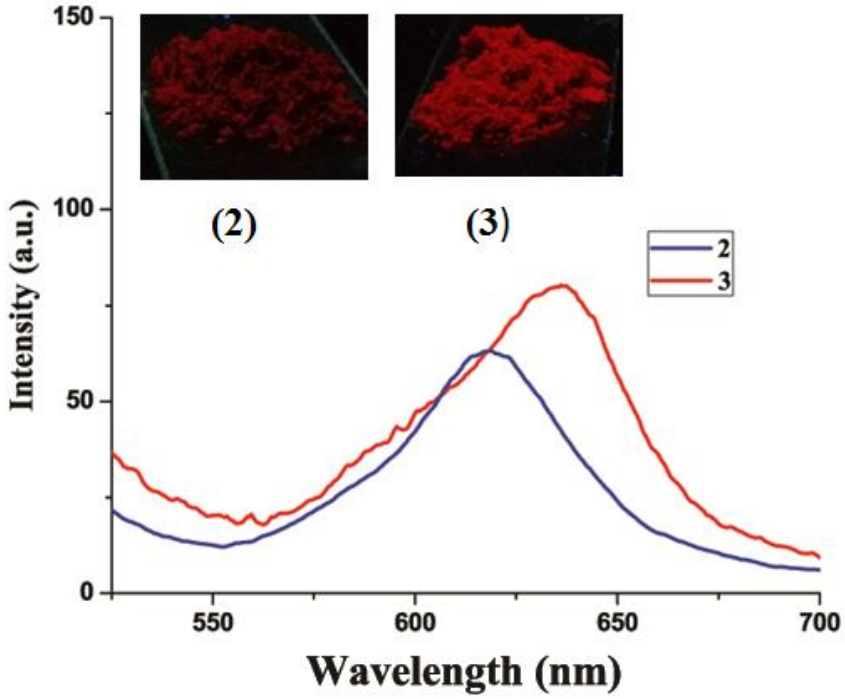

Fig. S15 Solid state emission spectra of **2-3**.

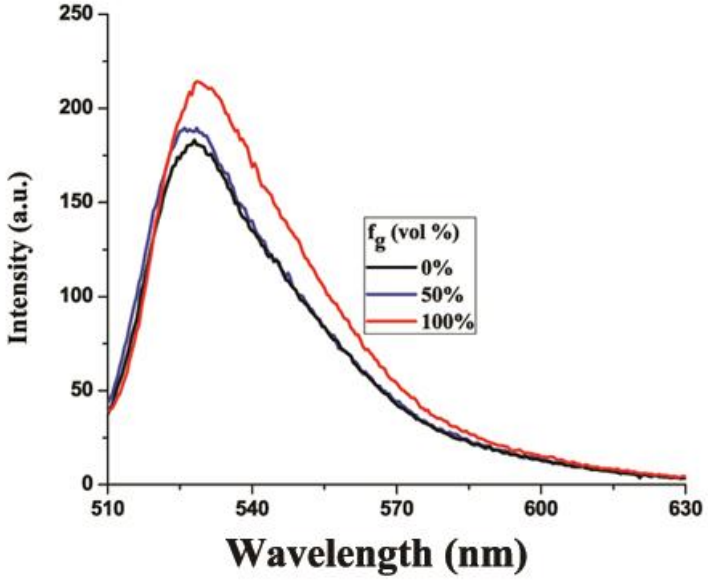

Fig. S16 Emission spectra of **1** in different fraction of glycerol.

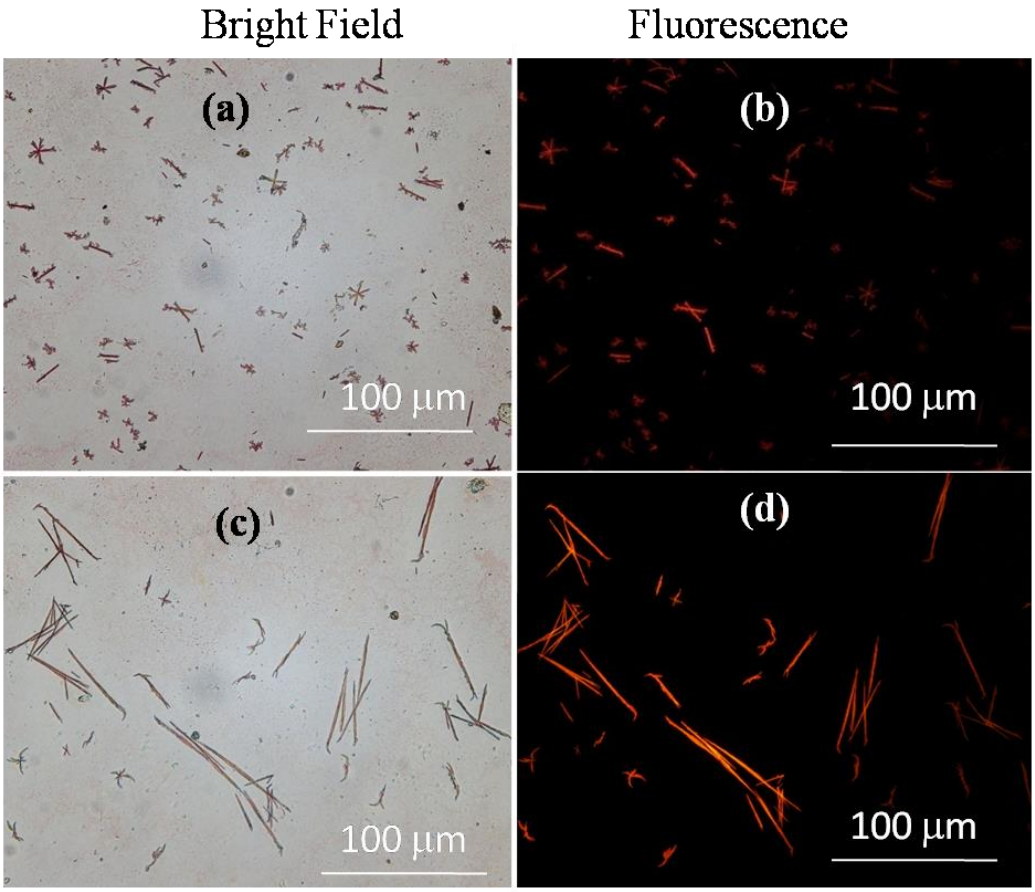

Fig. S17 Fluorescence optical microscope image of **2** (a, b) and **3** (c, d) at f_w 90% after 60 min of water injection.

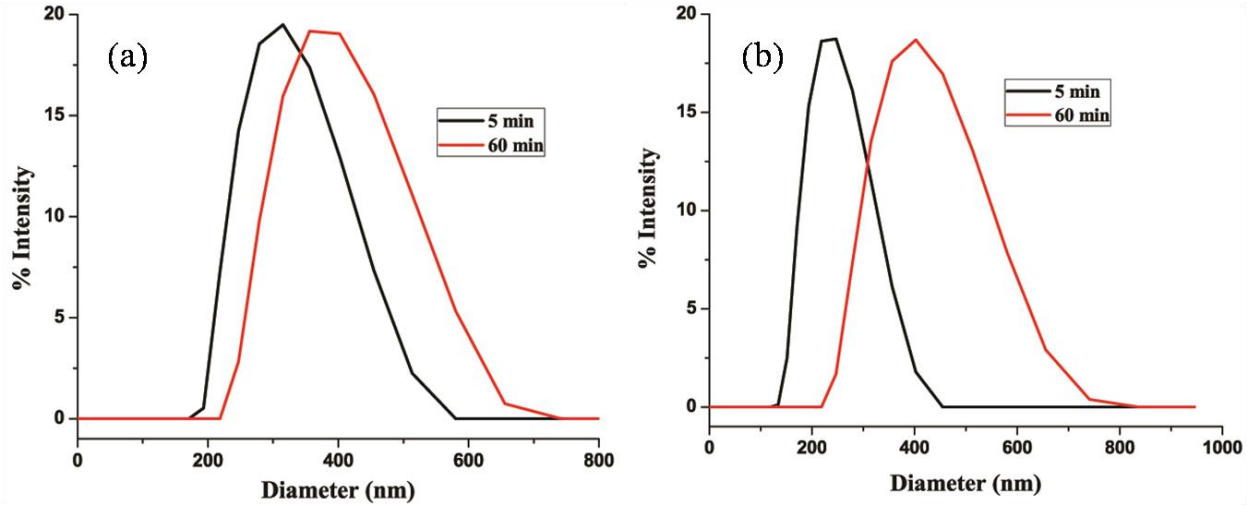

Fig. S18 DLS figures of **2** (a) and **3** (b) at f_w 90% at different time interval.

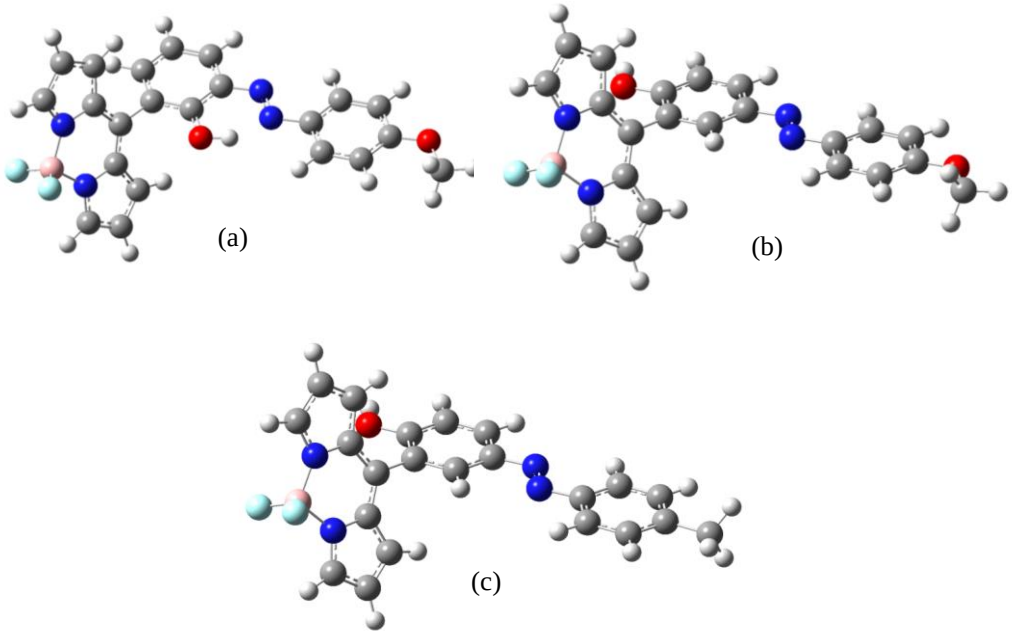

Fig. S19 DFT optimized figures of **1** (a), **2** (b) and **3** (c).

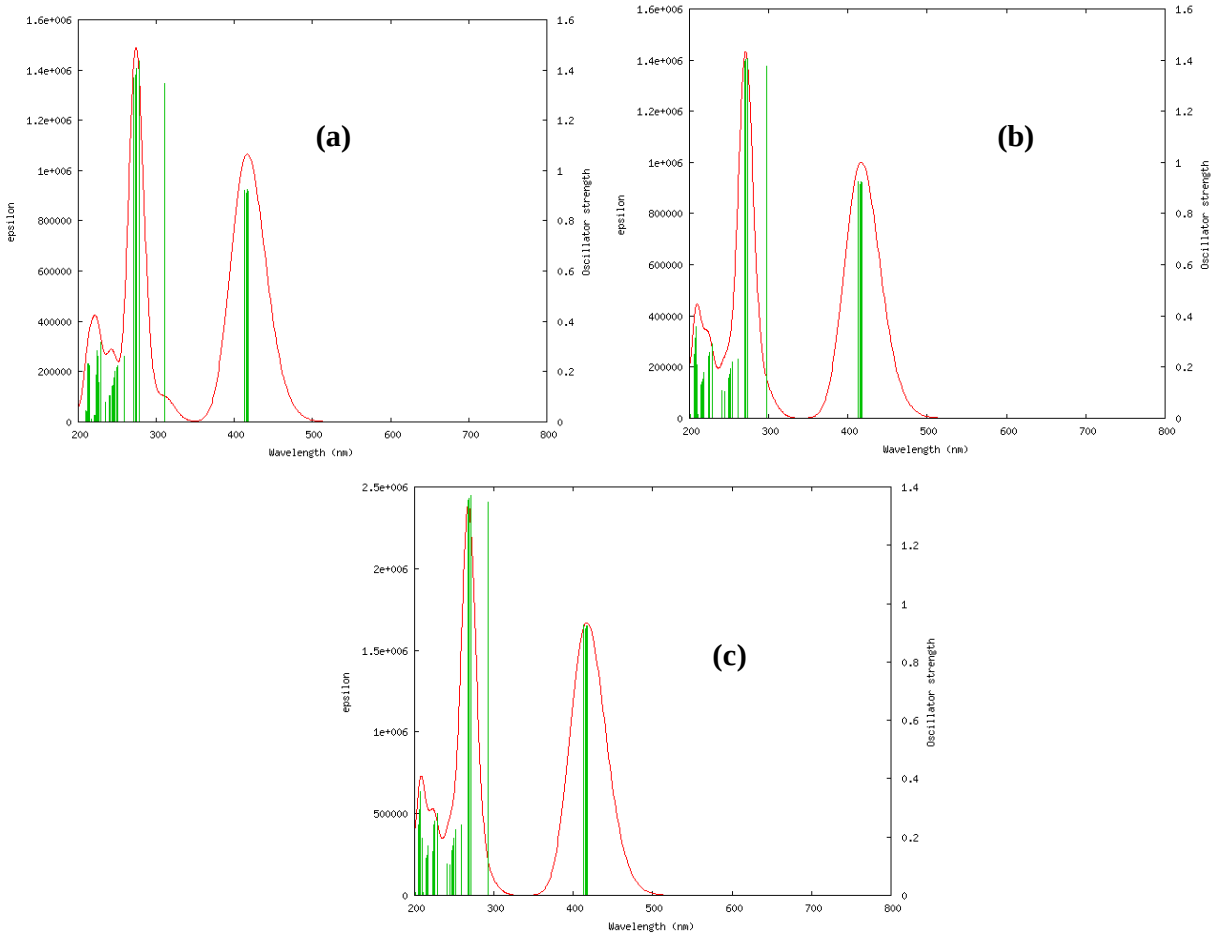

Fig. S20 UV–vis spectra of complexes **1** (a), **2** (b) and **3** (c) obtained from TD-DFT.

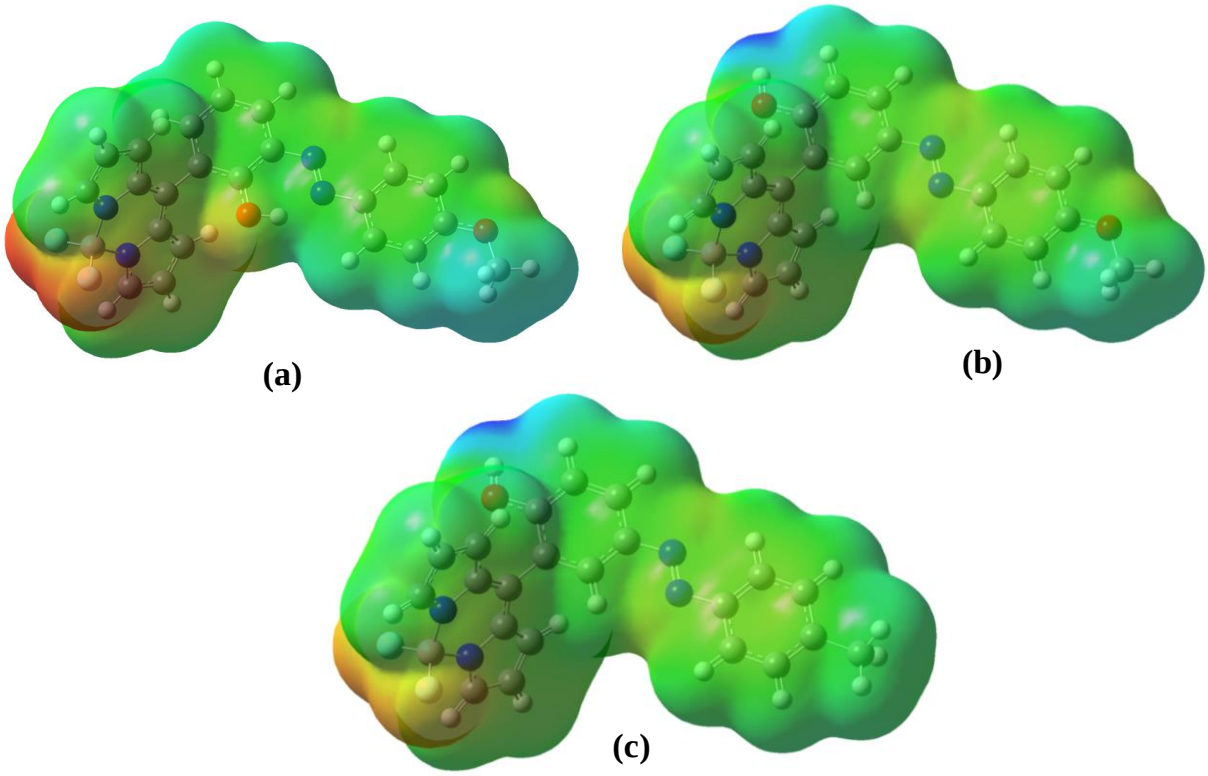

Fig. S21 Electrostatic potential surface of **1** (a), **2** (b) and **3** (c).

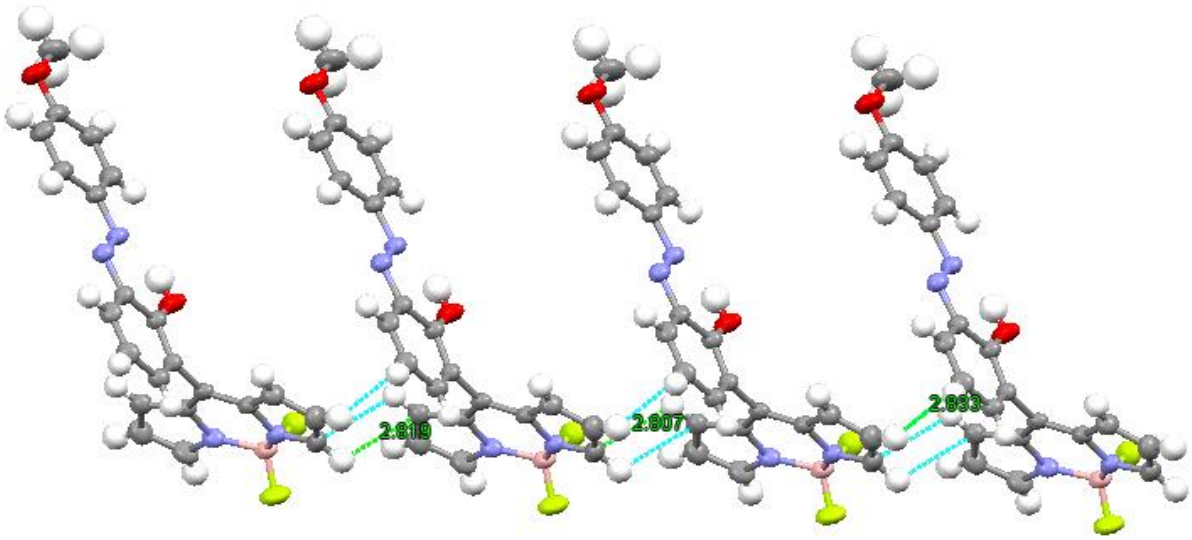

Fig. S22 Crystal packing showing C–H···π interactions in **1**.

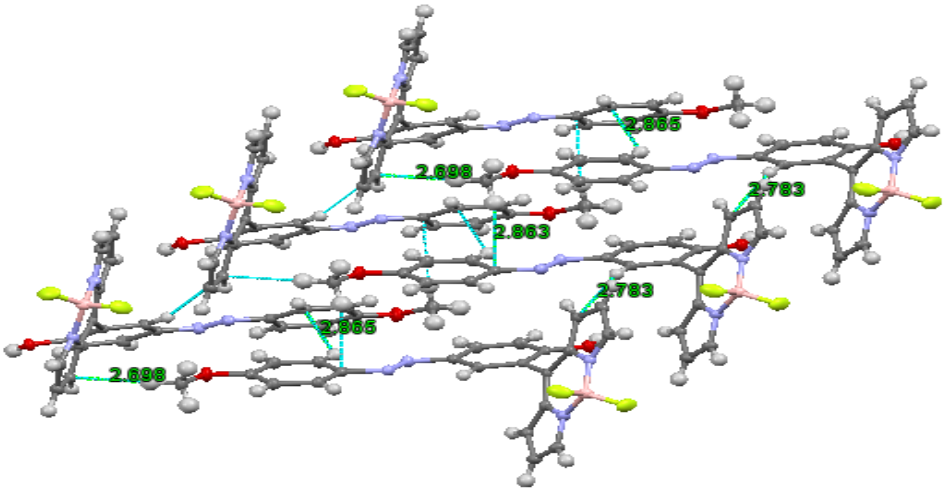

Fig. S23 Crystal packing showing C–H···π interactions in **2** (a).

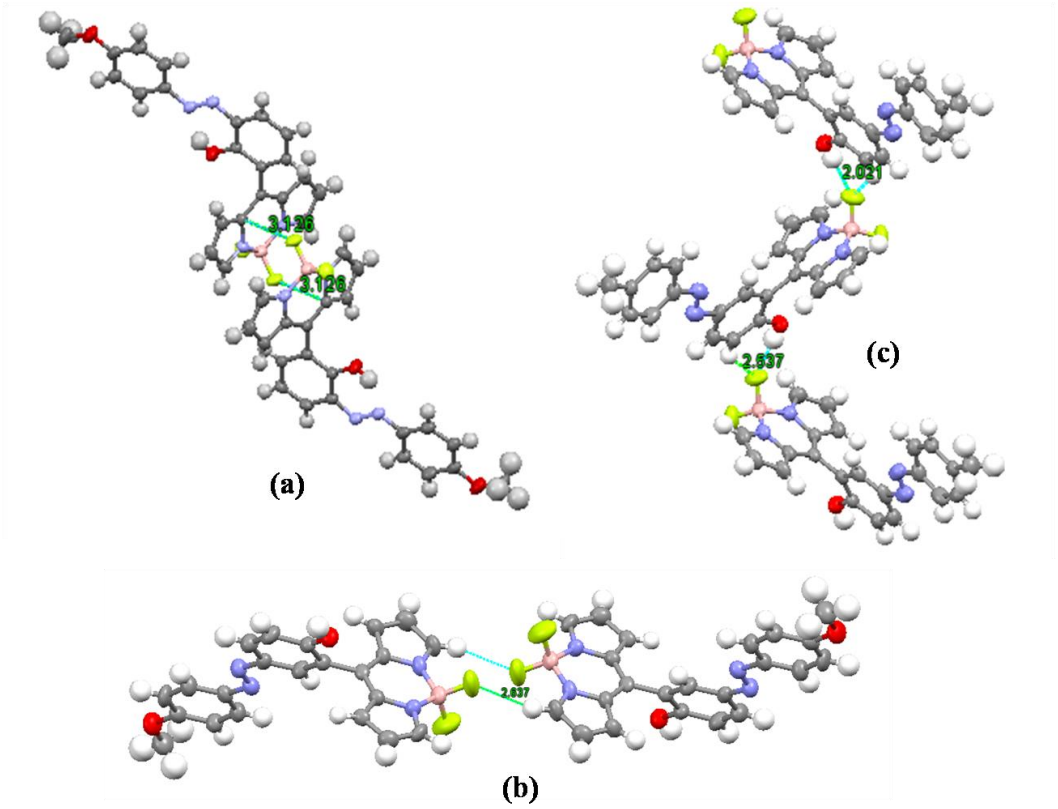

Fig. S24 Crystal packing showing C–H···F interactions in **1** (a), C–H···F in **2** (b), C–H···F and O–H···F in **3** (c).

Table S1: Selected bond distances in **1**–**3**.

Bond Length (Å)	**1**	**Bond Length (Å)**	**2**	**Bond Length (Å)**	**3**
N1–B1	1.539(2)	N1–B1	1.542(2)	N1–B1	1.533(3)
N2–B1	1.545(2)	N2–B1	1.543(13)	N2–B1	1.534(3)
N3–C12	1.4048(19)	N3–C12	1.4220(19)	N3–C14	1.425(4)
N4–C16	1.4132(19)	N4–C16	1.4283(19)	N4–C16	1.437(4)
N3–N4	1.2647(17)	N3–N4	1.2586(18)	N3–N4	1.248(4)
O1–C11	1.3456(17)	O1–C15	1.3540(18)	O1–C11	1.358(4)
O2–C19	1.3612(19)	O2–C19	1.3663(19)	C19–C22	1.496(6)

Table S2: Selected bond angles in **1**–**3**.

Bond Angle (°)	**1**	**Bond Angle (°)**	**2**	**Bond Angle (°)**	**3**
F1–B1–F2	109.13(13)	F1–B1–F2	108.47(13)	F1–B1–F2	108.67(17)
N2–B1–N1	105.65(12)	N2–B1–N1	106.62(11)	N2–B1–N1	106.52(15)
C16–C17–C21	119.20(14)	C21–C16–C17	119.21(14)	C21–C16–C17	119.2(3)
C13–C12–C11	119.12(13)	C13–C12–C11	118.98(13)	C13–C14–C15	119.0(2)
N3–C12–C11	124.91(13)	N3–C12–C13	115.52(13)	N3–C13–C14	112.9(3)
N4–C16–C21	124.18(14)	N4–C16–C17	116.50(13)	N4–C16–C21	116.8(3)
N4–N3–C12	115.42(12)	N4–N3–C12	115.15(12)	N4–N3–C14	113.8(3)
N3–N4–C16	116.19(12)	N3–N4–C16	114.04(12)	N3–N4–C16	115.6(3)

Table S3: Fluorescence quantum yields of **1–3**.

Compd	Φ_{soln}(%)	Φ_{solid}(%)
1	3	-
2	2.0	8
3	2.5	11

Φ_{soln} = fluorescence quantum yield in Methanol solution estimated using Rhodamine 6G as standard (Φ_F = 95% in water), Φ_{solid} = solid-state fluorescence (quantum yield determined by an calibrated integrating sphere.

Table S4: Fluorescence decay parameters of **2–3** in methanol solution and Methanol/water (1:9) mixture.

Methanol					**Methanol/water 1:9**			
Compd	λ (nm)	(A)	(τ) (ns)	<τ> (ns)	λ (nm)	(A)	(τ) (ns)	<τ> (ns)
2	525	40.6 (A_1) 8.00 (A_2) 51.37 (A_3)	2.62 (τ_1) 9.20 (τ_2) 0.39 (τ_3)	2	580	22.32 (A_1) 20.28(A_2) 57.40 (A_3)	4.12 (τ_1) 13.8 (τ_2) 0.32 (τ_3)	3.88
3	525	88 (A_1) 12 (A_2)	0.173 (τ_1) 8.18 (τ_2)	1.14	580	23.61 (A_1) 16.35 (A_2) 60.04 (A_3)	8.29 (τ_1) 17.14 (τ_2) 0.33 (τ_3)	4.95

Dynamic parameters determined from $I = A_1\exp(-t/\tau_1) + A_2\exp(-t/\tau_2) + y_0$, where A_1/A_2 and τ_1/τ_2 are the fractions (A) and lifetimes (τ) respectively. The weighted mean lifetime $<\tau>$ was calculated according to the equation: $<\tau> = (A_1\tau_1 + A_2\tau_2)/(A_1 + A_2)$. Solution concentration: 50 μM; excitation wavelength: 480 nm.

Table S5: Details of TD-DFT calculated electronic transitions for **1**–**3**.

Com	Exp. Wave length (nm)	Calcd. Wave length (nm)	Oscillator Strength (*f*)	Energy (ev)	% contibution	Important orbital excitation
1	501	412	0.92	3.00	94%	HOMO → LUMO
	362	310	1.346	3.99	86%	HOMO(–1) → LUMO(+1)
2	500	413	0.92	3.00	94%	HOMO → LUMO
	349	297	1.37	4.17	87%	HOMO(–1) → LUMO(+1)
3	502	413	0.92	3.00	95%	HOMO → LUMO
	351	292	1.34	4.23	88%	HOMO(–1) → LUMO(+1)